Hindawi
International Journal of Aerospace Engineering
Volume 2019, Article ID 1637953, 10 pages
https://doi.org/10.1155/2019/1637953

Research Article

Algorithm Used to Detect Weak Signals Covered by Noise in PIND

G. T. Wang,[1,2] X. W. Liang,[1] Y. Y. Xue,[1] C. Li,[2] and Q. Ding[1]

[1]*Electronic Engineering College of Heilongjiang University, Harbin 150008, China*
[2]*Institute of Electrical and Electronic Reliability, Harbin Institute of Technology, Harbin 150001, China*

Correspondence should be addressed to Q. Ding; 2247117478@qq.com

Received 3 June 2019; Revised 10 October 2019; Accepted 16 October 2019; Published 14 December 2019

Academic Editor: Ennes Sarradj

Detection of the loose particles is urgently required in the spacecraft production processes. PIND (particle impact noise detection) is the most commonly used method for the detection of loose particles in the aerospace electronic components. However, when the mass of loose particles is smaller than 0.01 mg, the weak signals are difficult to be detected accurately. In this paper, the aperiodic stochastic resonance (ASR) is firstly used to detect weak signals of loose particles. The loose particle signal is simulated by the oscillation attenuation signal. The influences of structure parameters on the potential height and detection performance of ASR are studied by a numerical iteration method. The cross-correlation coefficient C_1 between input and output is chosen as a criterion for whether there is an existing a particle or not. Through normalization, the loose particle signal-labeled high frequency of 135 kHz is converted into the low-frequency band, which can be detected by the ASR method. According to the algorithm, weak signals covered by noise could be detected. The experimental results show that the detection accuracy is 66.7%. This algorithm improves the detection range of weak loose particle signals effectively.

1. Introduction

Loose particles are impurities in aerospace electronic components, which is composed of metal debris, solder slag, conductor skin, etc. In a mechanical environment such as weightlessness and overweight, the loose particles are activated and released. The movable mechanism may be stuck due to the presence of the loose particles, and the action may be rejected. At the same time, the conductive loose particles may cause accidental conduction and malfunction and even lead to serious accidents in the aerospace electronic system. Therefore, the detection of loose particles is of great significance to the aerospace industry [1–3]. Because the loose particle is small and difficult to be detected, it requires high technology for weak signal detection.

At present, commonly used loose particle detection methods include microscopic observation, X-ray photography, MATRA detection, and remainder particle impact noise detection (PIND). PIND is widely applied for its fastness, convenience, low cost, and high sensitivity. The PIND method uses the sound signal generated by the collision between loose particles and the device wall to judge the existence of loose particles. The block diagram of the detecting device is shown in Figure 1. When the PIND test is carried out, the vibration table outputs the vibration and shock behaviors according to the default plan. The device to be tested is bonded to the sensor surface above the vibration table, which vibrates with the vibration table. The internal loose particle randomly collides with the inner wall of the tested device. The generated sound signal is received by the acoustic emission sensor. The detection waveform is transmitted to a voltage signal and output on the speaker and oscilloscope screen. After 50 years of development, PIND can detect loose particles with a mass of more than 0.01 mg, and the accuracy can reach 90%. However, PIND signals caused by the small particles whose mass is smaller than 0.01 mg are very weak and easily submerged in noise background, which makes it impossible to be detected [4–8].

Gao used the wavelet analysis to extract weak signals, and Wang et al. further introduced the stochastic resonance (SR)

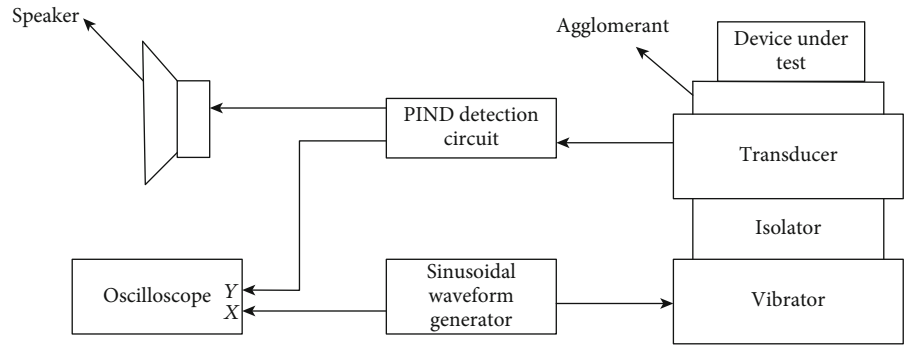

Figure 1: PIND system of MIL-STD-883E.

method, failing to extend the detection limit to 0.02 mg. Zhang used SR to process signals that cannot be extracted by the wavelet analysis, and the recognition probability is 12.5% [9].

In linear systems, "noise" is harmful. It destroys the stability, balance, order, certainty, and consistency of the system. It is the biggest obstacle that weakens signal detection. But in a nonlinear system, it is found that after data processing, the useful signal in the output is enhanced as the noise level increases, and the signal-to-noise ratio has been greatly improved, which has some synchronization. Analogous to the phenomenon of resonance in mechanical systems, it is called "stochastic resonance."

An SR system consists of weak signal input, noise input, and a nonlinear system for signal processing. The input signals can be periodic signals, aperiodic signals, random signals, etc. The input noises can be white noises, colored noises, etc.

Many scholars have done research related to the SR system. Li et al. used the method of rescaling frequency to solve large-parameter signals, and the improved SR was applied to fault diagnosis of mechanical equipment [10]. Initial research on SR was limited to the detection of periodic sinusoidal signals in the background of white noise using a nonlinear bistable system. That is, Benzi, an Italian scholar, used the phenomenon of "SR" in 1981 to study the nonlinear effects of ancient glaciers under the adiabatic approximation of bistable systems. The SR phenomenon in multistable systems driven by Gaussian noise was investigated theoretically and experimentally [11–13]. Many studies by using SR for weak signal detection have achieved positive research results [14–19]. But more signals are nonperiodic signals in practice [20]. Chow et al. put forward the concept of aperiodic stochastic resonance (ASR), which makes SR from theoretical research to practical application [21–24]. In this paper, the ASR method is used to detect the weak loose particle signals covered in the noise background for the first time.

In this paper, the characteristics of the ASR system are analyzed, and the cross-correlation coefficient is chosen as a criterion of the existence of loose particles. The relationship between structural parameters and potential height is obtained, and the effect of these parameters on the detection results are obtained through theoretical calculation. The weak loose particle signal covered in the noise is simulated with the oscillation attenuation signal with white noise. The relationship curve between the cross-correlation coefficient and the structure parameters is calculated numerically. By fine-tuning the structure parameters, when the cross-correlation coefficient is higher than the threshold value, it is determined that the experimental signal contains weak loose particle signals. The experimental results show that even if the particle signals are covered, noise can be detected. The detection accuracy is higher than 66.7%. This algorithm effectively improves the detection capability of weakly loose particles.

2. Aperiodic Stochastic Resonance Theory

2.1. Response and Characterization of Aperiodic Stochastic Resonance. A bistable Langevin model, which is sensitive to noise, is widely used in stochastic systems. The Langevin equation of the bistable system under the action of aperiodic signal $s(t)$ and Gauss white noise $\Gamma(t)$ is

$$\dot{x} = ax - bx^3 + s(t) + \Gamma(t), \quad a, b > 0 \langle \Gamma(t) \rangle = 0, \langle \Gamma(t), \Gamma(0) \rangle = 2D\delta(t). \tag{1}$$

Here, $\Gamma(t)$ is Gauss white noise whose mean is 0 and the intensity is D.

By using the concept of linear response, the system response function is defined as $\chi(\omega, D)$, which contains the response information of the weak signal input $s(t)$ and the noise information $\Gamma(t)$. Assuming that $s(t)$ and $x(t)$ are stationary Gauss stochastic processes, the cross-correlation function of input and output is assumed

$$K_{xs}(\tau) = \int_{-\infty}^{\infty} \int_{-\infty}^{\infty} x(t)s(t+\tau)P(x, t; s, t+\tau)dxds. \tag{2}$$

Here, $P(x, t; s, t+\tau)$ is the two-dimensional combined probability density of $s(t)$ and $x(t)$ for stochastic processes, and the cross-power spectral density $G_{xs}(\omega)$ is the Fourier transform of the cross-correlation function $K_{xs}(\tau)$.

$$G_{xs}(\omega) = \int_{-\infty}^{\infty} K_{xs}(\tau) \exp(-i\omega\tau)d\tau. \tag{3}$$

The definition of the coherence function is

$$\gamma^2(\omega) = \frac{|G_{xs}(\omega)|^2}{G_{xx}(\omega)G_{ss}(\omega)}. \tag{4}$$

The coherence function $\gamma(\omega)$ is a real number between 0 and 1. It can be used to describe the linear coherence degree of input $s(t)$ and output $x(t)$ in the frequency domain. The statistical characteristics of the weak signal $s(t)$ response of a nonlinear system can be calculated by the linear response theory, and the cross power spectral density $G_{xs}(\omega)$ can be expressed as

$$G_{xs}(\omega) = \chi(\omega, D)G_{ss}(\omega). \tag{5}$$

The power spectral density of output can be expressed as follows:

$$G_{xx}(\omega) = {G_{xx}}^{(0)}(\omega, D) + |\chi(\omega, D)|^2 G_{ss}(\omega). \tag{6}$$

Here, $G_{xx}^{(0)}(\omega, D)$ is the output power spectral density of nonlinear systems which is not disturbed by external aperiodic signals. Equations (5) and (6) are substituted with Equation (4); then

$$\gamma^2(\omega) = 1 - \frac{{G_{xx}}^{(0)}(\omega, D)}{{G_{xx}}^{(0)}(\omega, D) + |\chi(\omega, D)|^2 G_{ss}(\omega)}. \tag{7}$$

From Equation (7), the coherence function is less than 1 and varies with the noise intensity D. When the noise intensity is optimized, the consistency between input and output increases and the coherence function increases. The coherence function is the characterization quantity describing the consistency of ASR input and output in the frequency domain. Assuming that the system input is $s(t)$ and the output is $x(t)$, the covariance C_0 of the input and output is defined as

$$C_0 = \left\langle \left[s(t) - \bar{s(t)}\right]\left[x(t) - \bar{x(t)}\right]\right\rangle. \tag{8}$$

Therefore, the cross-correlation coefficient C_1 is defined as follows:

$$C_1 = -\frac{C_0}{\sqrt{\left\langle \left[x(t) - \bar{x(t)}\right]^2\right\rangle \left\langle \left[s(t) - \bar{s(t)}\right]^2\right\rangle}}. \tag{9}$$

From the signal processing point of view, maximizing C_1 is equivalent to maximizing the matching degree between input and output. C_0 and C_1 can also be calculated by $G_{xs}(\omega)$, $G_{ss}(\omega)$, and $G_{xx}(\omega)$, and the following relationships are established:

$$\begin{aligned} C_0 &= \int_0^\infty \mathrm{Re}\,(G_{xs}(\omega))d\omega, \\ C_1 &= C_0\left[\int_0^\infty G_{ss}(\omega)d\omega \int_0^\infty G_{xx}(\omega)d\omega\right]^{-1/2}. \end{aligned} \tag{10}$$

ASR's linear response theory and cross-correlation description are applied to bistable systems. Assuming that the aperiodic input $s(t)$ is a Gaussian noise signal, the correlation time is τ_0, and the root mean square value is Q, the input power spectrum is

$$G_{ss}(\omega) = \frac{Q\tau_0}{1 + \omega^2 {\tau_0}^2}. \tag{11}$$

According to the linear response theory, the expressions of $G_{xx}^{(0)}(\omega, D)$ and $\chi(\omega, D)$ are as follows: when only the inter-well transition is considered, the single exponential term is approximated, and there is no external disturbance.

$$\begin{aligned} {G_{xx}}^{(0)}(\omega, D) &= \frac{2\lambda_m \langle x^2\rangle_{st}}{{\lambda_m}^2 + \omega^2}, \\ \chi(\omega, D) &= \frac{1}{D}\frac{\lambda_m \langle x^2\rangle_{st}}{{\lambda_m}^2 + \omega^2}(\lambda_m - i\omega). \end{aligned} \tag{12}$$

Here, λ_m is the minimum of nonzero eigenvalue corresponding to the Fokker-Planck operator, which is related to the Kramers transition rate r_K.

$$\lambda_m = 2r_K = \frac{\sqrt{2}a}{\pi}\exp\left(-\frac{\Delta V}{D}\right). \tag{13}$$

In the undisturbed nonlinear bistable system, the steady-state value of the two order matrix is $\langle x^2\rangle_{st}$. Equation (12) are substituted with Equation (7), and the expression of the coherence function is obtained [25].

$$\gamma^2(\omega) = 1 - \left(1 + \frac{\lambda_m \langle x^2\rangle_{st}}{D^2}\frac{Q\tau_0}{1 + \omega^2 {\tau_0}^2}\right). \tag{14}$$

And the cross-correlation coefficient C_1 is also obtained at the same time.

$$C_1 = \left[\left(\frac{\lambda_m\tau_0}{1 + \lambda_m\tau_0}\right)\left(1 - \frac{D^2(1 + \lambda_m\tau_0)}{D^2(1 + \lambda_m\tau_0) + Q\lambda_m\tau_0\langle x^2\rangle_{st}}\right)\right]^{1/2}. \tag{15}$$

In Equation (15), $a = 1$, $b = 1$, and $Q = 0.01$, 10, and 20 for τ_0, respectively, and the curve of C_1 with D is shown in Figure 2. The variation curve of C_1 with D shows a peak, indicating that ASR occurs in a bistable system. The greater the correlation time of input noise, the higher the matching degree between output and input. Therefore, the use of bistable ASR can detect weak aperiodic signals [26].

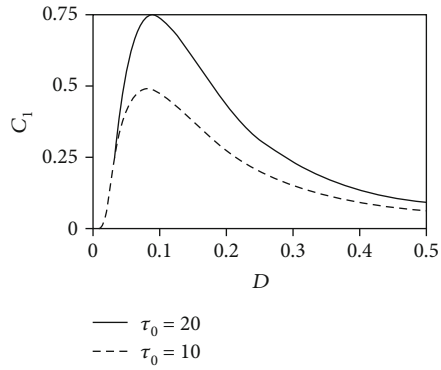

Figure 2: The curve of C_1 with D.

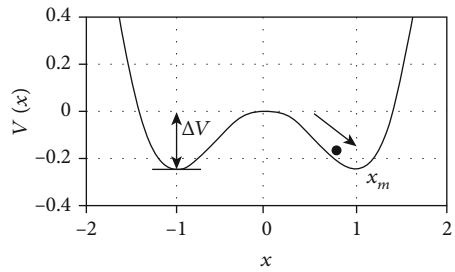

Figure 3: The bistable system potential well.

2.2. Mechanism of Stochastic Resonance. The bistable stochastic resonance system for Equation (1) is a non-self-excited system, and the potential function is

$$U(x) = -\frac{a}{2}x^2 + \frac{b}{4}x^4, \quad a > 0,\ b > 0. \tag{16}$$

When $a = 1$ and $b = 1$ are available, it can be represented in Figure 3. The diagram contains two potential wells under the bistable system, and ΔV indicates potential height.

Assuming that it reaches the critical value of double-well SR driven by a signal with $A_{\min}$ amplitude, the potential function $U(x)$ satisfies

$$\begin{aligned} \frac{\partial U}{\partial x} &= -ax + bx^3 + A_{\min}, \\ \frac{\partial^2 U}{\partial x^2} &= -a + 3bx^2 = 0. \end{aligned} \tag{17}$$

From Equation (17), the threshold $A\sqrt{4a^3/27b}_{\min}$ of the input signal is obtained; that is to say, when the input signal amplitude $A \geq \sqrt{4a^3/27b}$, the system can generate double potential well SR.

When the input signal strength A and the noise intensity D are not zero, the original equilibrium of the bistable system will be broken and the potential well will be tilted. When the input amplitude is larger than the threshold value, bistable SR will occur; otherwise, special intrawell resonance will occur, which is called "single potential well approximation model under bistability." When there is only noise $\Gamma(t)$ and no periodic excitation, the particle transits between two potential wells according to Kramers transition rate r_K. r_K depends on the distribution and intensity of noise. The expression is as follows:

$$r_K = \frac{a}{\sqrt{2}\pi} \exp\left(-\frac{\Delta V}{D}\right). \tag{18}$$

For the periodic signal of the input system, the bistable potential well will periodically tilt under its driving and produce SR, whose frequency is the same as that of the input signal; for the nonperiodic signal of the input system, the bistable potential well will also tilt and produce ASR.

3. Establishment of the Bistable Stochastic Resonance System

Bistable systems in SR can be represented by the Langevin equation, which has been described in detail in Section 2.1 of this paper. When SR is applied to the detection of weak loose particle signals, practical problems such as the form of loose particle signal and noise and the adjustment of system parameters need to be considered.

3.1. The Model of the Particle Signal. Loose particle signal is a typical random and aperiodic signal. The single pulse signal collected in the experiment is the oscillating attenuation signal, which is shown in Figure 4(a)). It can be simulated in the following equation [27]:

$$u(t) = A_0 \exp\left(-\frac{t}{k}\right) \sin(2\pi f t). \tag{19}$$

Here, A_0 is the maximum amplitude of the input signal, k is the impact attenuation coefficient, and f is the oscillation frequency. Setting the parameters to $A_0 = 1.25$, $k = 1.5$, and $f = 5$ can simulate the pulse particle signal, as shown in Figure 4(b).

To more realistically simulate the actual weak signal of the loose particle, the Gauss white noise with root mean square $\sigma = 1$ is superimposed on the above model, and the mixed signal $v(t)$ is obtained as shown in Figure 5. At this point, the loose particle signal has been completely covered by the noise.

3.2. Influence of Structural Parameters on the System. In the process of synergistic effect among signal, noise, and nonlinear systems, potential height and SR peak will change with system structure parameters. This paper analyzes the influence of system parameters a and b on the system and output employing simulation. The qualitative explanation of stochastic resonance is given by using a Langevin equation based on simplification and constraints when uncertainties such as noise are ignored. In this paper, SR is quantitatively analyzed by numerical simulation.

Equation (1) is a nonlinear stochastic differential equation, which can be solved only by numerical methods. Based on the Runge-Kutta algorithm, this paper adopts a

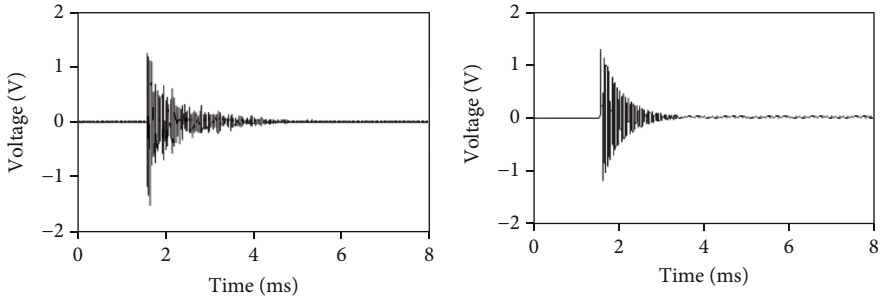

(a) The real particle pulse signal (b) The simulated particle pulse signal

Figure 4: The real particle pulse signal and its simulating signals.

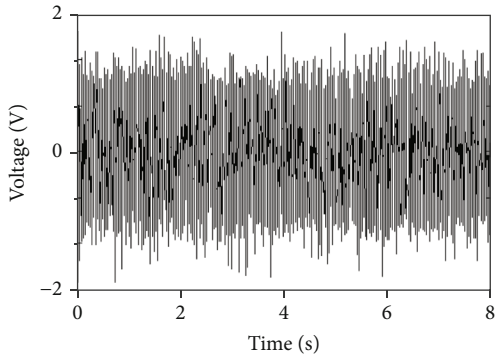

Figure 5: The simulated particle pulse signal with noise.

numerical iteration algorithm for solving nonlinear stochastic differential equations [28, 29].

$$
\begin{aligned}
x_{n+1} &= x_n + \frac{1}{6}(k_1 + 2k_2 + 2k_3 + k_4),\\
k_1 &= h\left[ax_n - bx_n^3 + sn_n\right],\\
k_2 &= h\left[a\left(x_n + \frac{k_1}{2}\right) - b\left(x_n + \frac{k_1}{2}\right)^3 + sn_n\right],\\
k_3 &= h\left[a\left(x_n + \frac{k_2}{2}\right) - b\left(x_n + \frac{k_2}{2}\right)^3 + sn_n\right],\\
k_4 &= h\left[a(x_n + k_3) - b(x_n + k_3)^3 + sn_n\right].
\end{aligned}
\tag{20}
$$

Here $h = 1/f_s$ is the simulation step, f_s is the sampling frequency, sn_n is the nth sampling point of the input signal with noise, and x is the output signal. To prevent the divergence of iteration, the simulation condition of the bistable system SR is

$$
ah \le 1, \quad |x_0| \le \sqrt{\frac{ah + 2}{bh}}. \tag{21}
$$

The results show that the sampling frequency has a great influence on the stability of the system output and SR effect. Generally, the sampling frequency is selected to be more than 50 times of the target detection signal frequency.

3.2.1. Effect of a and b on Detection Performance. According to Equations (17), the structural parameters a and b of the system have a direct impact on the input threshold of the system. When the input signal amplitude is less than $A_{\min}$, the single potential well SR will occur in the bistable state; otherwise, the bistable SR will occur.

The maximum amplitude $A_0 = 1.25$, attenuation coefficient $k = 1.5$, oscillation frequency $f = 5$, and noise variance $D = 2.5$ are selected in the model $u(t) = A_0 \exp(-(t/k))\sin(2\pi f t)$ of particle signal. At this time, the signal to noise ratio of the input signal is very low, and the particle signal is completely annihilated by noise. The influence of a and b on SR is also studied utilizing control variables, and the potential height and the distance between two wells increase with the increase of a and decrease with the increase of b.

C_1 is chosen as the characterization parameter to describe the detection performance. Here, we set $b = 0.8$ to study a as an example to discuss. When $a = 50$, the system input and output time-frequency diagram is shown in Figure 6.

Since the loose particle signal is a high-frequency signal in most instances, the SR system can only process the low-frequency signal, so the input high signal needs to be normalized; therefore, the obtained output signal is 0~1 Hz. High-frequency signal processing will be explained in Section 3.3.

Compared with Figures 6(a) and 6(c), when $a = 50$ and $b = 0.8$, the output of the system cannot clearly show the characteristics of the input signal, whether in the time domain or frequency domain. Therefore, resonance does not occur because the parameters a and b are not selected properly. Keep the input signal amplitude and noise intensity unchanged, and gradually reduce the value of a. When a is set as 11 and 3, respectively, the output time-frequency diagrams are shown in Figures 7 and 8.

Compared with Figures 6–8, the SR system can extract the loose particle effectively when a is set as 11 and 3, respectively, and the output waveform is closer to the input signal when $a = 3$ than when $a = 11$. It can be concluded that in Figures 7 and 8, due to the reasonable selection of parameters, resonance can be generated and the loose particle signal can be detected. However, since the input time domain signal peak value is at time 0, we get the output frequency domain signal as well and the maximum peak value

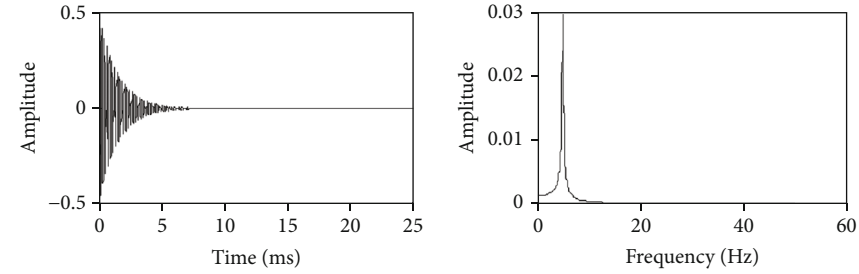

(a) The time and frequency spectrum of particle signal

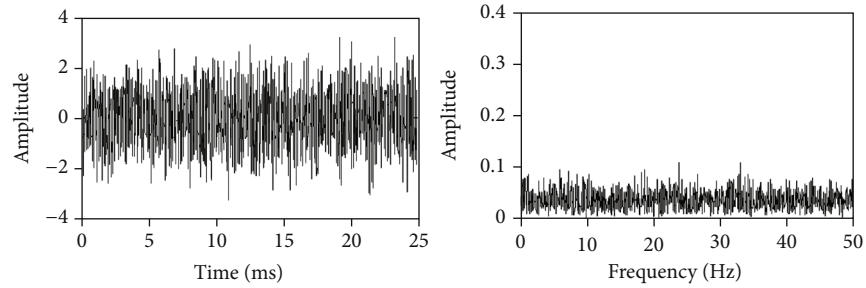

(b) The time spectrum and frequency of particle signal with noise

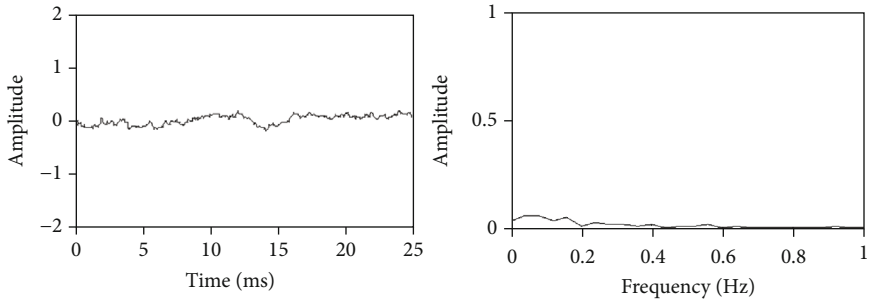

(c) The time and frequency spectrum of system output

Figure 6: The time and frequency spectrum of the system input and output when $a = 50$ and $b = 0.8$.

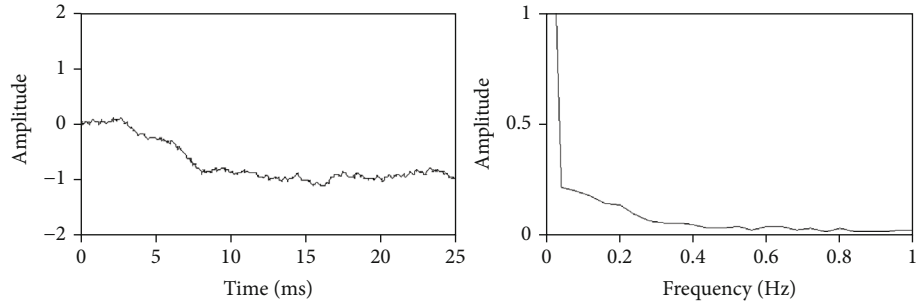

Figure 7: The time and frequency spectrum of the system input and output when $a = 11$ and $b = 0.8$.

at time zero. As shown in Figure 9, the parameter b is fixed, and the variation of C_1 with the parameter a is calculated and the curve is drawn.

3.3. High-Frequency Signal Processing. The Langevin equation describes the Brownian motion of particles in a fluid, which is the most concise model in the bistable system. The research on the characteristics of SR systems is also mainly dependent on them. According to the SR system described by the model, the Fokker-Planck equation of Equation (22) can be established to analyze the effect of noise on the system.

$$\frac{\partial \rho(x,t)}{\partial t} = -\frac{\partial}{\partial x}\left[(A\cos 2\pi f t)\rho(x,t)\right] + D\frac{\partial^2}{\partial x^2}\rho(x,t). \quad (22)$$

Because of the time-dependent term $-(\partial/\partial x)[(A\cos 2\pi f t)\rho(x,t)]$ in the Fokker-Planck equation, the equation can only be approximately solved. The approximate

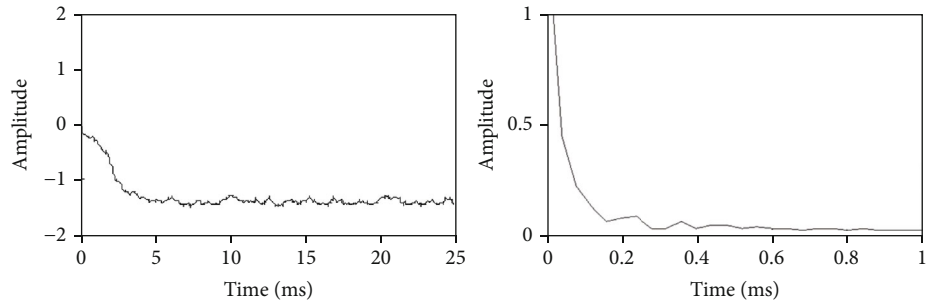

Figure 8: The time and frequency spectrum of the system input and output when $a = 3$ and $b = 0.8$.

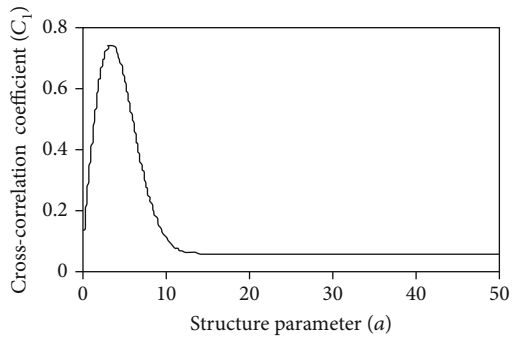

Figure 9: The relationship between the cross-correlation coefficient C_1 and the structure parameter a.

method is the adiabatic approximation theory. Adiabatic approximation theory is the earliest, most systematic, and persuasive approximation theory for describing periodic SR systems. Its application condition is that the signal frequency is far less than the transition rate ($2\pi f << r_K$); that is, SR can only process low-frequency signals. However, there are a lot of high-frequency signals in the project, and the particle pulse is about 135 kHz of the narrowband modulation signal. How to deal with high-frequency signal is the key problem of ASR in the loose particle signal detection.

The amplitude of the weak signal is A and the frequency is $\omega >> 1$. The dynamic model of the bistable system is

$$\dot{x} = ax - bx^3 + A\sin(\omega t + \varphi) + N(t). \quad (23)$$

Equation (23) is transformed into a normalized form, and variable substitution $z = x\sqrt{b/a}$, $\tau = at$ is introduced.

$$a\sqrt{\frac{a}{b}}\frac{\mathrm{dz}}{\mathrm{dt}} = a\sqrt{\frac{a}{b}}z - a\sqrt{\frac{a}{b}}z^3 + A\cos\left(\frac{\omega}{a}\tau\right) + N\left(\frac{\tau}{a}\right). \quad (24)$$

Here, $N(\tau/a)$ satisfies $E[N(\tau/a)N(0)] = 2Da\delta(\tau)$ and defines $\varepsilon(\tau)$ as Gauss white noise of intensity 0.5; that is $E[\varepsilon(\tau)] = 0, E[\varepsilon(\tau)\varepsilon(0)] = \delta(\tau)$, and Equation (24) is shown as follows:

$$\frac{dz}{d\tau} = z - z^3 + \sqrt{\frac{b}{a^3}}A\cos\left(\frac{\omega}{a}\tau + \varphi\right) + \sqrt{\frac{2Db}{a^2}}\varepsilon(\tau). \quad (25)$$

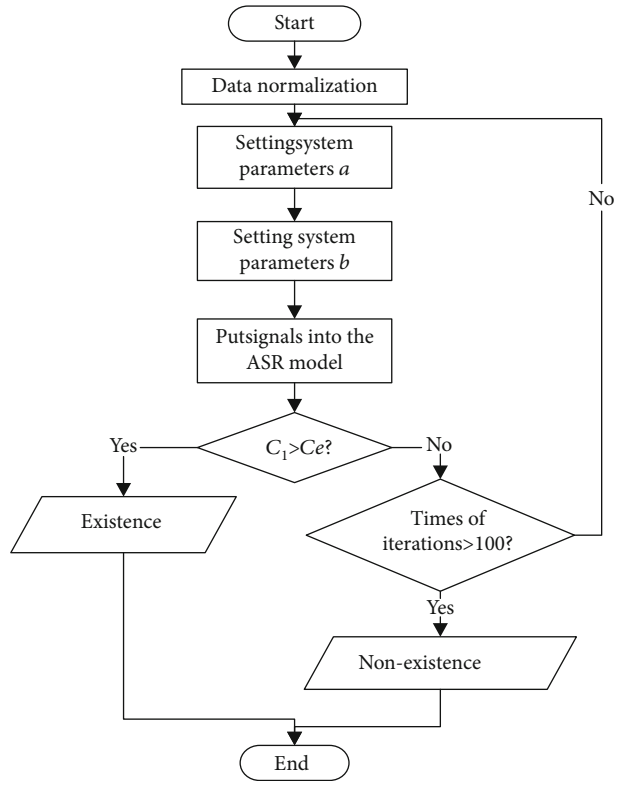

Figure 10: The flow chart of the algorithm for weak particle signal based on ASR.

Equation (25) is the normalized form of Equation (23). The normalized signal's frequency becomes $1/a$ of the original signal frequency, which satisfies the hypothesis of the adiabatic approximation theory. Therefore, a large parameter a can be selected for high-frequency signals to meet the requirements of the SR theory.

3.4. The Detection Algorithm for the Weak Particle Signal. Based on the above analysis, this paper presents a detection algorithm for the weak loose particle signal based on ASR. Its flow chart is shown in Figure 10.

The main steps are as follows:

(1) Signal normalization: the particle signal with noise is normalized to [-1,1] through amplitude and scale transformation, and its frequency is changed into the reciprocal to satisfy the constraints of ASR on frequency

(2) Parameter a selection: according to the law of the loose particle pulse signal width, select the appropriate parameter a. For example, when the pulse width of the loose particle signal is generally concentrated in $T = 10\mu s - 100\mu s$, the priority is to set a to $1/T$ of 3-10 times, that is, 30000-1000000

(3) Parameter b selection: parameter b and parameter a are generally in the same order of magnitude or an order of magnitude different; according to the experience, the value of b is slightly smaller than that of a

(4) The input is substituted for the ASR model to solve the problem. The output results are analyzed, and the cross-correlation coefficient C_1 is calculated to determine whether the set threshold is reached. If not, the parameters are fine-tuned according to the actual situation; then the solution is brought in again until the threshold is reached, and the existence of remainder particle is determined. If the threshold is not reached after 100 iterations, there is no particle. A threshold can be counted by the results of many simulation experiments, and the C_1 interval with good output for detection can be obtained. Set the minimum value of the interval to be the threshold value, that is, Ce = 0.35

4. Experimental Verification

Considering that the current loose particle detection equipment has a poor detection effect on the weak signal generated by the loose particle of less than 0.01 mg, this is because the signal is too weak and it is covered by noise. In this paper, a tin-containing loose particle with a mass of about 0.01 mg is implanted into 10 models of relays and 5 transistor cavities of a certain type: 100 tests for each group of subjects. The ASR algorithm is used to process the collected acoustic emission signals. Since the frequency of the loose particle signal is about 135 kHz, according to Section 3.3 the analysis of the parameter setting of the high-frequency signal processing by the SR system, we can conclude that the bistable system needs to normalize the high frequency loose particle signal to make its frequency become $1/a$ of the original signal frequency. So we set parameter a to 800000 and parameter b to 50000. In each experiment, the frequency of the input signal fluctuated slightly, so the parameters a and b need to be fine-tuned on a set basis for each experiment. The original input signal is the noise-containing loose particle signal that is amplitude-shifted, scale-scaled, and normalized into the interval [-1,1]. The experimental results are shown in Table 1, and the cross-correlation coefficient is the average of 100 experimental results. The threshold of the cross-correlation coefficient is calculated by the results of multiple simulation experiments, and it is found that it can detect the C_1 interval with good output. The minimum value of the interval is set to the threshold Ce; finally, the threshold Ce is set to 0.35 according to the simulation experiment results.

Table 1: The cross-correlation coefficient was received by averaging 100 tests.

No.	Package types	Particle	C_1	Result
1	1/5 crystal cover	0.01 mg tin grain	0.0993	Nonexistent
2	1/5 crystal cover	0.01 mg tin grain	0.2952	Nonexistent
3	1/5 crystal cover	0.01 mg tin grain	0.6410	Existent
4	1/5 crystal cover	0.01 mg tin grain	0.5545	Existent
5	1/2 crystal cover	0.01 mg tin grain	0.6716	Existent
6	1/2 crystal cover	0.01 mg tin grain	0.4590	Existent
7	1/2 crystal cover	0.01 mg tin grain	0.0250	Nonexistent
8	TO-5	0.01 mg tin grain	0.5944	Existent
9	TO-5	0.01 mg tin grain	0.6538	Existent
10	TO-5	0.01 mg tin grain	0.4751	Existent
11	TO-3	0.01 mg tin grain	0.5304	Existent
12	TO-3	0.01 mg tin grain	0.5202	Existent
13	TO-3	0.01 mg tin grain	0.2746	Nonexistent
14	TO-3	0.01 mg tin grain	0.4588	Existent

Experiment results show that the weak loose particle signal can be detected very well.

As shown in the table, after repeating experiments for 100 times, 10 of the 15 relays with loose particles could accurately detect the existence of particle. The experimental results show that the weak loose particle signal detection algorithm based on ASR can improve the detection level to a certain extent, and the accuracy rate is 66.7%. Moreover, different package types also influence the results of the test. As can be seen in Table 1, the TO-5 package has higher accuracy than the other two packages, probably because the structure of this package is simpler.

5. Discussion

We introduced a loose particle signal detection algorithm based on the aperiodic stochastic resonance (ASR) system for detecting nonperiodic high-frequency signals and showed this achieved higher classification accuracy. In this study, we can detect the loose particle signal less than 0.01 mg that was not detected before; in other words, the weak loose particle signal is completely covered by the noise signal, which is theoretically and practically meaningful. In our experiment with 15 aerospace relays containing 0.01 mg of the loose particle, we observed that although the signal is completely covered by noise, it can be detected by the method of this paper and the accuracy of the detection obtained is higher than other methods. The main reasons why some aerospace relays cannot be accurately detected are as follows:

(1) Because the input signal amplitude is too small, the system has SR in the well, which results in the change of system characteristics, the "synergistic effect" is affected, and the output characteristics become worse

(2) Due to the unreasonable selection of parameters a and b, SR is difficult to extract in the system driven by weak signals

(3) Due to the large Ce setting of the threshold, some of the data that have occurred in SR have been misjudged as nonredundant objects

In future experiments, while we are working hard to solve the above problems, we should also pursue higher speeds and parameter tuning. We can also use other algorithms to improve the classification accuracy and reduce the error rate.

6. Conclusions

In this paper, an ASR system for detecting weak signals is constructed, and the loose particle signal is simulated by oscillating the attenuation signal. The influence of structure parameters on the potential height and detection performance of ASR is studied by the numerical iteration method. Through simulation, the relationship curves between the cross-correlation coefficient C_1 and structure parameters are obtained. By normalization, the 135 kHz high-frequency loose particle signal is converted into the low-frequency band, which can be detected by the ASR method. According to the algorithm, a loose particle weak signal detection with a mass of 0.01 mg is performed, with an accuracy of 66.7%. This algorithm improves detecting weak loose particle signal range from 0.02 mg to 0.01 mg effectively and can detect signals that are completely covered by noise.

Data Availability

The data used in this experiment were obtained from the aerospace sealing relay, so it involved a certain degree of confidentiality. At the same time, our institute signed a confidentiality agreement with the production unit, so the data could not be released.

Conflicts of Interest

The authors declare that there is no conflict of interest regarding the publication of this paper.

Acknowledgments

This work was cosupported by the National Natural Science Foundation of China (Nos. 51607059, 51077022, and 61271347), Natural Science Foundation of Heilongjiang Province (QC2017059), Postdoctoral Fund in Heilongjiang Province (LBH-Z16169), Talent Innovation Special Project of Heilongjiang Province (HDRCCX-201604), Science and Technology Innovative Research Team in Higher Educational Institutions of Heilongjiang Province (No. 2012TD007), and Heilongjiang University Youth Science Fund Project (QL201505).

References

[1] P. Roettjer, "Testing techniques to improve relay reliability," *Evaluation Engineering*, vol. 44, no. 4, pp. 44–48, 2005.

[2] G. Zhai, J. Chen, S. Wang, K. Li, and L. Zhang, "Material identification of loose particles in sealed electronic devices using PCA and SVM," *Neurocomputing*, vol. 148, pp. 222–228, 2015.

[3] R. Chen, S. Wang, G. Zhai, and S. Yi, "A feature extraction method for remnant particles based on non-negative tensor factorization in aerospace electronic equipments," in *2012 IEEE International Instrumentation and Measurement Technology Conference Proceedings*, pp. 1650–1653, Graz, Austria, 2012.

[4] D. A. Jackson, "Tools and techniques for area relay coordination studies," in *57th Annual Conference for Protective Relay Engineers, 2004*, pp. 220–246, College Station, TX, USA, 2004.

[5] J. L. Angleton and S. L. Webster, "Techniques for Standardization of Particle Noise in Electronic Packages," *12th Annual Proceedings of Reliability Physics*, no. 7, pp. 38–42, 1994.

[6] S.-j. Wang, H.-l. Gao, and G.-f. Zhai, "Research on feature extraction of remnant particles of aerospace relays," *Chinese Journal of Aeronautics*, vol. 20, no. 3, pp. 253–259, 2007.

[7] D. Ivanov, M. Ovchinnikov, and M. Sakovich, "Relative Pose and Inertia Determination of Unknown Satellite Using Monocular Vision," *International Journal of Aerospace Engineering*, vol. 2018, Article ID 9731512, 9 pages, 2018.

[8] X. Ying, W. Liu, G. Hui, and J. Fu, "E-nose based rapid prediction of early mouldy grain using probabilistic neural networks," *Bioengineered*, vol. 6, no. 4, pp. 222–226, 2015.

[9] Z. Long, *Research on particles detection and identification system for aerospace power, [M.S. thesis]*, Harbin Institute of Technology, 2010.

[10] J. Li, X. Chen, and Z. He, "Multi-stable stochastic resonance and its application research on mechanical fault diagnosis," *Journal of Sound and Vibration*, vol. 332, no. 22, pp. 5999–6015, 2013.

[11] S. Lu, Q. He, and J. Wang, "A review of stochastic resonance in rotating machine fault detection," *Mechanical Systems and Signal Processing*, vol. 116, pp. 230–260, 2019.

[12] D. Han, P. li, S. An, and P. Shi, "Multi-frequency weak signal detection based on wavelet transform and parameter compensation band-pass multi-stable stochastic resonance," *Mechanical Systems and Signal Processing*, vol. 70-71, pp. 995–1010, 2016.

[13] P. Shi, P. Li, S. An, and D. Han, "Stochastic resonance in a multistable system driven by Gaussian noise," *Discrete Dynamics in Nature and Society*, vol. 2016, Article ID 1093562, 7 pages, 2016.

[14] L. Gammaitoni, P. Hänggi, P. Jung, and F. Marchesoni, "Stochastic resonance," *Reviews of Modern Physics*, vol. 70, no. 1, pp. 223–287, 1998.

[15] B. E. Klamecki, "Use of stochastic resonance for enhancement of low-level vibration signal components," *Mechanical Systems and Signal Processing*, vol. 19, no. 2, pp. 223–237, 2005.

[16] Y. Hakamata, Y. Ohno, K. Maehashi, S. Kasai, K. Inoue, and K. Matsumoto, "Enhancement of weak-signal response based on stochastic resonance in carbon nanotube field-effect transistors," *Journal of Applied Physics*, vol. 108, no. 10, article 104313, 2010.

[17] J. Tan, X. Chen, J. Wang et al., "Study of frequency-shifted and re-scaling stochastic resonance and its application to fault diagnosis," *Mechanical Systems and Signal Processing*, vol. 23, no. 3, pp. 811–822, 2009.

[18] H. Niaoqing, C. Min, and W. Xisen, "The application of stochastic resonance theory for early detecting rub-impact fault of rotor system," *Mechanical Systems and Signal Processing*, vol. 17, no. 4, pp. 883–895, 2003.

[19] X. Ying, H. Lin, and G. Hui, "Study on non-linear bistable dynamics model based EEG signal discrimination analysis method," *Bioengineered*, vol. 6, no. 5, pp. 297-298, 2015.

[20] R. Benzi, A. Sutera, and A. Vulpiani, "The mechanism of stochastic resonance," *Journal of Physics A: Mathematical and General*, vol. 14, no. 11, pp. 453–457, 1981.

[21] C. C. Chow, T. T. Imhoff, and J. J. Collins, "Enhancing aperiodic stochastic resonance through noise modulation," *Chaos: An Interdisciplinary Journal of Nonlinear Science*, vol. 8, no. 3, pp. 616–620, 1998.

[22] C. Bai, "Time delay effects of stochastic resonance induced by multiplicative periodic signal in the gene transcriptional regulatory model," *Physica A: Statistical Mechanics and its Applications*, vol. 507, pp. 304–311, 2018.

[23] P. Jia, J. Yang, H. Liu, and E. Hu, "Improving amplitude-modulated signals by re-scaled and twice sampling vibrational resonance methods," *Pramana*, vol. 91, no. 3, p. 38, 2018.

[24] C. Wan, M. Pan, Q. Zhang, F. Wu, L. Pan, and X. Sun, "Magnetic anomaly detection based on stochastic resonance," *Sensors and Actuators A: Physical*, vol. 278, pp. 11–17, 2018.

[25] Y. Dingxin, *Stochastic Resonance Method and Application Research of Weak Feature Signal Detection*, Graduate School of National University of Defense Technology, 2004.

[26] G. P. Harmer and D. Abbott, "Simulation of circuits demonstrating stochastic resonance," *Microelectronics Journal*, vol. 31, no. 7, pp. 553–559, 2000.

[27] G. Hongliang, *Research on automatic detection and feature recognition method for space relay reminder, [Ph.D. thesis]*, Harbin Institute of Technology, 2007.

[28] D. Han, X. Su, and P. Shi, "Stochastic resonance in multi-stable system driven by Levy noise," *Chinese Journal of Physics*, vol. 56, no. 4, pp. 1559–1569, 2018.

[29] G. Hui, J. Zhang, J. Li, and L. Zheng, "Sucrose quantitative and qualitative analysis from tastant mixtures based on cu foam electrode and stochastic resonance," *Food Chemistry*, vol. 197, pp. 1168–1176, 2016.